Multipath Benefits of BOC vs. BPSK Modulated Signals Using On-Air Measurements

Chiawei Lee, Yu-Hsuan Chen, Gabriel Wong,
Sherman Lo, and Per Enge, *Stanford University*

BIOGRAPHIES

Chiawei Lee is a Flight Test Engineer at the Air Force Test Center at Edwards AFB, CA where he performs systems integration on a variety of USAF and international platforms. He received his M.S. in Aero/Astro Engineering from Stanford University, where he is a student researcher, and B.S. in Aerospace Engineering from UCLA. His research interests include multipath mitigation and anti-jam/anti-spoofing methods and technologies.

Yu-Hsuan Chen, Ph.D., is a Postdoctoral Scholar in the GPS Laboratory at Stanford University. He received his Ph. D. in Electrical Engineering from National Cheng Kung University, Taiwan in 2011. His research interests include real-time GNSS software receiver design and its application to antenna-array beam-forming, dual frequency and multipath analysis.

Gabriel Wong is an Electrical Engineering Ph.D. candidate at the Stanford University GNSS Research Laboratory. He has previously received an M.S.(EE) from Stanford University, and a B.S.(EECS) from UC Berkeley. His current research involves signal deformation monitoring and mitigation for GNSS signals.

Sherman Lo, Ph.D., is currently a senior research engineer at the Stanford GPS Laboratory. He is the Associate Investigator for the Stanford University efforts on the FAA evaluation of alternative position navigation and timing (APNT) systems for aviation. He is a recipient of the ION Early Achievement Award.

Per Enge, Ph.D., is a professor of aeronautics and astronautics at Stanford University, where he is the Kleiner-Perkins Professor in the School of Engineering. He directs the GNSS Research Laboratory, which develops satellite navigation systems. He has been involved in the development of the Federal Aviation Administration's GPS Wide Area Augmentation System (WAAS) and Local Area Augmentation System (LAAS). For this work, Enge has received the Kepler, Thurlow, and Burka awards from the Institute of Navigation (ION). He received his Ph.D. from the University of Illinois. He is a member of the National Academy of Engineering and a Fellow of the IEEE and the ION.

ABSTRACT

Binary Offset Carrier (BOC) modulated signals are currently being used in the Galileo E1 signal and will be used in the future GPS L1C signal. BOC modulation allows for improved multipath performance by narrowing the correlation peak when compared to the BPSK modulation used in the current GPS L1 C/A signal. Multipath effects can be further reduced through the use of composite BOC (CBOC) and time-multiplexed BOC (TMBOC) modulation.

This paper presents a methodology and results from collecting and assessing CBOC, BOC(1,1), and Binary Phase Shift Keying (BPSK) multipath performance using a software-defined receiver and a commercial antenna. In contrast to previous work, which focuses primarily on simulated multipath envelopes or tracking algorithms for CBOC/BOC, the methodology in this paper is used to assess and compare multipath performance using collected field measurements. It compares the pseudorange precision of CBOC, BOC(1,1), and BPSK in various scenarios chosen for their expected multipath characteristics.

The data collection hardware was mobilized to allow the research team to gather data outside of the lab; in scenarios which more closely mimic the real-world conditions experienced by ground based GNSS users. In total, five scenarios were tested including: 1) open-sky (reference), 2) rooftop, 3) courtyard, 4) urban canyon, and 5) under foliage.

INTRODUCTION

Multipath is a substantial component in the error budget of current GPS receiver systems. As shown in Figure 01, errors in today's single frequency are dominated by ionospheric effects. However, tomorrow's multi-frequency systems will see multipath as the dominant error source, as shown in Figure 02 [01].

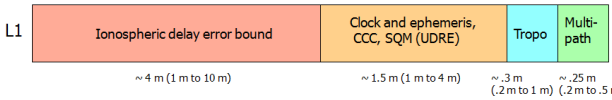

Figure 01: Ionospheric delay as the primary error source in single frequency receivers

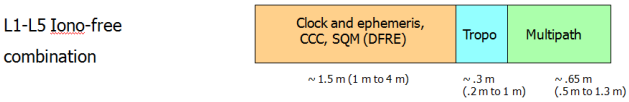

Figure 02: Multipath as the primary error source in dual frequency receivers

Signal design is one means of mitigating multipath. A wider band signal results in narrower correlation peaks resulting in lower multipath susceptibility. Binary Offset Carrier (BOC) modulated signals by design have narrower correlation peaks. The steeper slope of the correlation peak yields improved signal tracking performance. BOC modulated signals are currently being used in the Galileo In-Orbit Validation (IOV) satellites and will be used in the future GPS III constellation.

Signal tracking performance can be further improved through the use of Multiplexed BOC (MBOC) spreading modulation. Composite BOC (CBOC) uses a weighted sum of BOC(1,1) and BOC(6,1) to form a composite signal. This is the approach used by the Galileo system. In contrast, GPS III will use Time-Multiplexed BOC (TMBOC) which combines BOC(6,1) and BOC(1,1) in the time dimension [02]. The higher frequency segment of either MBOC modulation technique creates a portion of the signal with even steeper correlation peaks.

Figure 03 [02] shows the multipath error envelope as a function of multipath delay for binary phase shift keying (BPSK), BOC(1,1), and TMBOC. The envelope for CBOC is similar to TMBOC as shown in the figure. It can be observed that BOC(1,1) provides an advantage to BPSK for delays greater than approximately 450 nanosecond (ns) and CBOC/TMBOC provides an advantage for delays greater than 75ns.

The signals compared in our study were CBOC(6,1,1/11) (hereto referred to simply as CBOC), BOC(1,1) (hereto referred to simply as BOC), and BPSK(1) (hereto referred to simply as BPSK). TMBOC was not evaluated due to the lack of actual signals being transmitted from satellites currently in orbit.

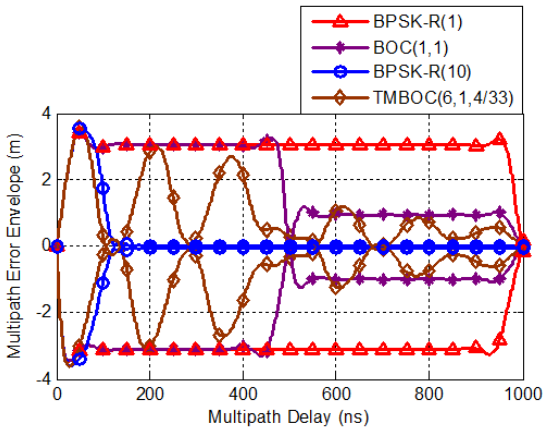

Figure 03: Multipath error envelope comparison as a function of multipath delay

Though much previous work has been accomplished detailing the theoretical or simulated performance benefits of BOC, CBOC, and/or TMBOC, there is a lack of results coming from actual field measurements. To contribute to this gap, the authors devised a series of experiments which used pseudorange precision as a way of measuring multipath in various geometries and scenarios (described in a later section).

MULTIPATH CALCULATION METHODOLOGY

Multipath affects the signal to varying degrees based on receiver bandwidth and how far the correlators are spaced. Greater multipath errors are seen on the wider correlator spacings [03].

A COTS USRP receiver was specially configured to provide 5 tracking loops per channel. For each channel, each tracking loop is set at a different correlator spacing (0.1, 0.2, 0.3, 0.4, 0.5 chips), and provides a different pseudorange [04], as described in equations 01-05.

Equations for pseudoranges [**5**]:

$$\rho_{0.1} = r + c[\delta t_u - \delta t^s] + I_\rho + T_\rho + \varepsilon_{\rho,0.1} + MP_{\rho,0.1} \quad (01)$$

$$\rho_{0.2} = r + c[\delta t_u - \delta t^s] + I_\rho + T_\rho + \varepsilon_{\rho,0.2} + MP_{\rho,0.2} \quad (02)$$

$$\rho_{0.3} = r + c[\delta t_u - \delta t^s] + I_\rho + T_\rho + \varepsilon_{\rho,0.3} + MP_{\rho,0.3} \quad (03)$$

$$\rho_{0.4} = r + c[\delta t_u - \delta t^s] + I_\rho + T_\rho + \varepsilon_{\rho,0.4} + MP_{\rho,0.4} \quad (04)$$

$$\rho_{0.5} = r + c[\delta t_u - \delta t^s] + I_\rho + T_\rho + \varepsilon_{\rho,0.5} + MP_{\rho,0.5} \quad (05)$$

Where

ρ:	*Pseudorange*
r:	*True range*
c:	*Speed of light*
δt_u:	*User clock bias in seconds*
δt^s:	*Satellite clock bias in seconds*
I_ρ:	*Ionospheric error in pseudorange domain, in meters*

T_ρ: *Tropospheric error in pseudorange domain, in meters*

ε_ρ: *Receiver thermal noise error in pseudorange domain, in meters. Although different for the different tracking loops, the errors are small and dominated by multipath.*

$MP_{\rho,0.1}$: *Multipath error pseudorange domain in meters; (tracking loop of 0.1 chip correlator spacing)*

$MP_{\rho,0.2}$: *Multipath error pseudorange domain in meters; (tracking loop of 0.2 chip correlator spacing)*

$MP_{\rho,0.3}$: *Multipath error pseudorange domain in meters; (tracking loop of 0.3 chip correlator spacing)*

$MP_{\rho,0.4}$: *Multipath error pseudorange domain in meters; (tracking loop of 0.4 chip correlator spacing)*

$MP_{\rho,0.5}$: *Multipath error pseudorange domain in meters; (tracking loop of 0.5 chip correlator spacing)*

For the same channel, the true range and troposphere and ionosphere errors in the pseudorange equations are common-mode for the tracking loops of different correlator spacings. The receiver clock bias is also common mode due to the use of a common clock. Thus, performing single-differences between the pseudoranges leaves the multipath and receiver noise errors and removes all other common mode errors. For the test environments of interest, multipath errors are generally much larger than receiver noise especially after smoothing. The other correlator-spacing dependent error, nominal signal deformation, is also dominated by multipath for these test cases. Thus the single-differenced pseudoranges show the magnitude of the multipath effects.

In order to measure the multipath-induced errors and compare the results from CBOC, BOC, and BPSK, the receiver hardware and software was mobilized and brought to several locations on campus (described in a later section). At each location, data was gathered for approximately 10 minutes (limited by data storage space).

For the experiments described in this paper, the pseudorange from the narrowest correlator spacing of 0.1 chips (set by receiver limitations) was used as the reference as it had the lowest noise. All single-differenced pseudoranges were obtained by differencing the pseudoranges from wider correlator spacings with this reference. This allowed us to obtain the single-differenced pseudoranges which can be used to quantify the magnitude of multipath effects.

IMPORTANCE OF CORRELATOR SPACING

The placement of correlators along the correlation function is critically important to the signal tracking performance. Because tracking sensitivity is a function of the local slope at the particular correlator spacing chosen, it is important to place correlators at points where the slope is steepest. Figure 04 shows the correlation peak comparison between BPSK, BOC(1,1), CBOC, and TMBOC [06]. It is clear that at all points, BOC, CBOC, and TMBOC are steeper than BPSK. However, the comparison between BOC and CBOC/TMBOC is not as clear-cut.

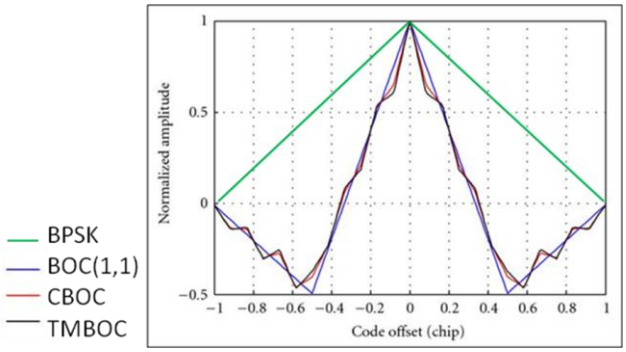

Figure 04: Comparison of correlation peaks of BPSK, BOC(1,1), CBOC, and TMBOC

Figure 05 shows a zoomed in view of Figure 04 at three example correlation spacings. At a correlator spacing of 0.1 chips (correlators at +/- 0.05 chips), both CBOC and TMBOC correlation function slopes are steeper than the BOC slope. However, at a correlator spacing of 0.5 chips (a natural choice to most), the slope for both CBOC and TMBOC is in fact shallower than BOC. Placing CBOC/TMBOC correlators here would yield worse signal tracking performance compared to BOC. For this paper, the narrowest correlator achievable by receiver limitations (0.1 chips) was used as a reference. The wide correlator was placed at 0.4 chips in order to take advantage of the steeper local slope of the CBOC correlation function.

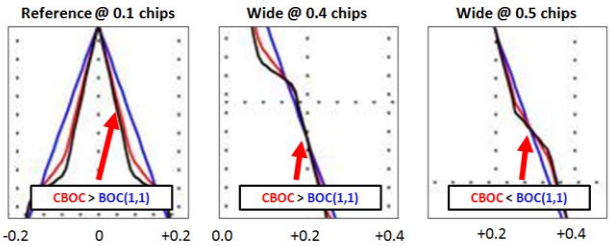

Figure 05: Comparison of the correlation peak local slopes of BOC(1,1), CBOC, and TMBOC

HARDWARE/SOFTWARE RECEIVER DESCRIPTION

The data collection and analysis system used a survey grade antenna and an in-house, multiple channel software receiver, which enabled the research team to collect data from both types of satellites (Galileo IOV and GPS) using the same hardware at the same time. The software receiver was also developed to provide simultaneous ranging outputs at several correlator spacings. Multipath effects are time-varying in nature; in addition non-

constant hardware biases may be present. Using simultaneous measurements protected us from both these additional sources of measurement noise.

Description of Signal Collection Hardware and Experimental Setup

The hardware used to collect the antenna array datasets is depicted in Figure 06. The hardware contained two Trimble Zephyr antennas, two USRP2 software radio systems and one host computer. The signal received from the antenna passed to a USRP2 board equipped with a DBSRX2 programmable mixing and down-conversion daughterboard. The individual USRP2 boards were synchronized to a common frequency by a 10 MHz external common clock generator and triggered by a common Pulse per Second (PPS) signal. The USRP2s were controlled by a host computer running the Ubuntu distribution of Linux. The open-source GNU Radio software-defined radio block was used to configure the USRP2 and collect the dataset. All USRP2s were configured to collect signals at L1 (1575 MHz).

The signals were converted to near zero Intermediate Frequency (IF) and digitized to 14-bit complex outputs (I & Q). Its sampling rate was set as 20 MHz and the host computer used two solid state drives for storing the data set. As recording the high bandwidth signal requires a high data stream rate of (80 MB/sec/antenna), fast solid state drives were used for this study

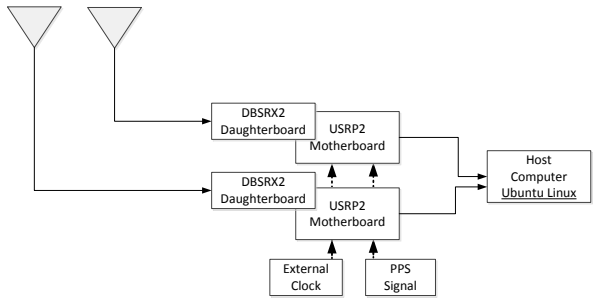

Figure 06: Block diagram of the signal collection hardware

Description of Software Receiver

The software was developed using the Eclipse software development environment under the 64-bit version of Ubuntu shown in Figure 07; most source codes were programmed using C++. The functionalities with high computational complexity, such as correlation operation, were programmed by assembly. The IF data were read from the disk and amplified by automatic gain control to equalize the noise power. Then, it was processed in parallel through several software receiver channels using software correlators with different correlator spacings and signal-processing/acquisition-to-tracking engines. The software correlator adopts Single Instruction, Multiple Data (SIMD) instruction [07]. The software correlator was controlled by a signal-processing function for setting PRN, code phase, and Doppler frequency. The signal-processing used the correlator outputs to decide the channel state from acquisition to tracking [08]. Finally, the pseudoranges were measured and written to a log file.

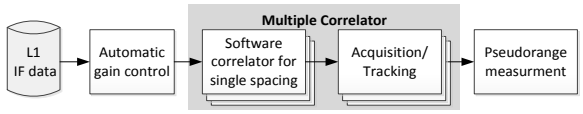

Figure 07: Block diagram of software receiver

EXPERIMENT SETUP/MULTIPATH SCENARIOS

Experiments were set up in order to collect data at a time when a pair of satellites (Galileo IOV and GPS) was at similar azimuth and elevation in order to minimize the errors induced by the ionosphere and troposphere. Common error sources such as clock and hardware biases were also eliminated by the use of the same receiver hardware collecting data for all satellites simultaneously. This setup also allowed for data collection from multiple pairs of satellites during the same experiment period.

Five scenarios were chosen for their varying multipath characteristics. All locations are on the campus of Stanford University, Stanford, CA.

1) Open-Sky (reference): Data collected in the middle of Lake Lagunita, a dry-lake bed, provided a clean reference signal.
2) Rooftop: Data collected on the roof of the Durand Building provided a scenario where there was one primary direction of multipath.
3) Courtyard: Data collected on the rooftop courtyard of the Durand Building provided a scenario mimicking a pedestrian, walking environment.
4) Urban Canyon: Data collected between buildings in the Engineering Quad provided a scenario mimicking an urban, driving environment.
5) Under Foliage: Data collected in the New Guinea Sculpture Garden provided a scenario mimicking environments under a canopy of foliage.

Pictures from each of the scenarios are shown in Figure 08.

Figure 08: Scenarios chosen based on expected multipath performance

In addition, data were collected from three different satellite pairs, each consisting of one Galileo IOV satellite and one GPS satellite.

1) Galileo PFM & GPS PRN 25
2) Galileo FM2 & GPS PRN 2
3) Galileo FM2 & GPS PRN 26

Skyplots showing the satellite geometries during the data collection time windows is shown in Figure 09.

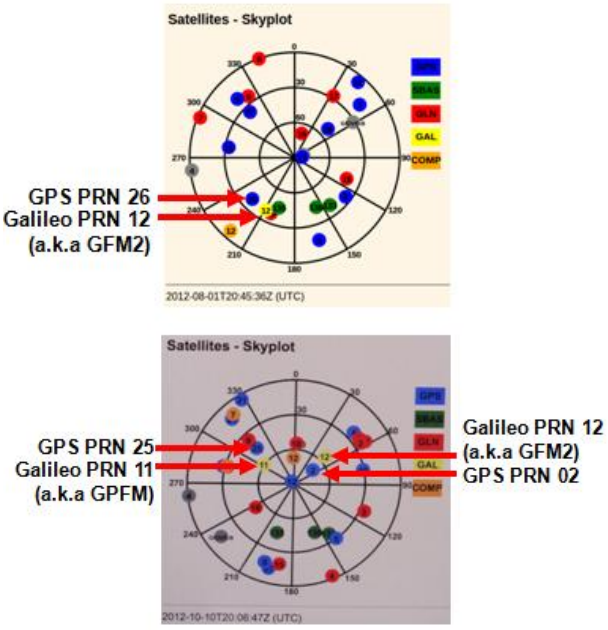

Figure 09: Data are collected from satellite pairs based on similar geometry

RESULTS AND DISCUSSION

As shown in Figures 10, in a clear sky environment, there is little to no advantage gained by CBOC or BOC modulation over BPSK. However, in more challenging multipath environments, CBOC and BOC modulation provides a measureable performance gain over BPSK. Figure 11 shows the pseudorange precision errors in a simple multipath environment on the rooftop courtyard of the Durand Building. The multipath measured from the CBOC/BOC signals were approximately half that of the BPSK signal.

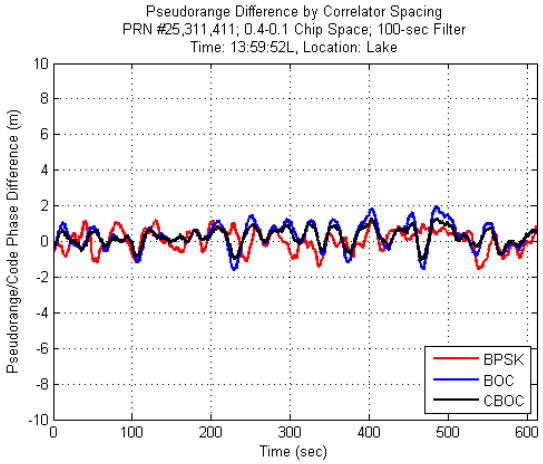

Figure 10: Multipath error comparison between CBOC, BOC, and BPSK under open skies

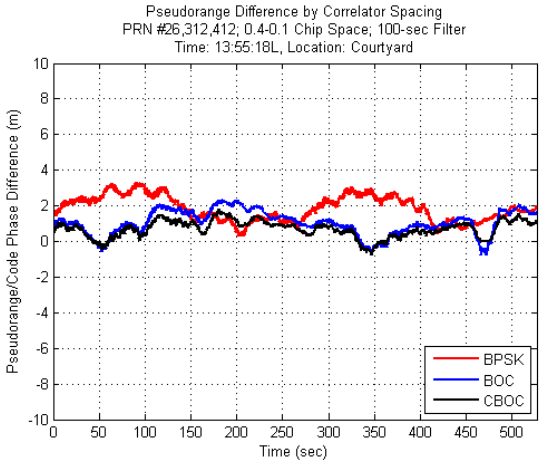

Figure 11: Multipath error comparison between CBOC, BOC, and BPSK from the rooftop courtyard

Since it is impossible to attain a perfect geometry match between the GPS and Galileo satellites, it is more meaningful to compare the multipath measured from the CBOC and BOC signals. Those results come from the same signal with the only difference being the higher frequency portion of the replica contained in the CBOC receiver channel. Similar to Figure 11 in the rooftop courtyard, the results from Figure 12 showed that

multipath errors in the CBOC signal are always less than the multipath errors in the BOC signal.

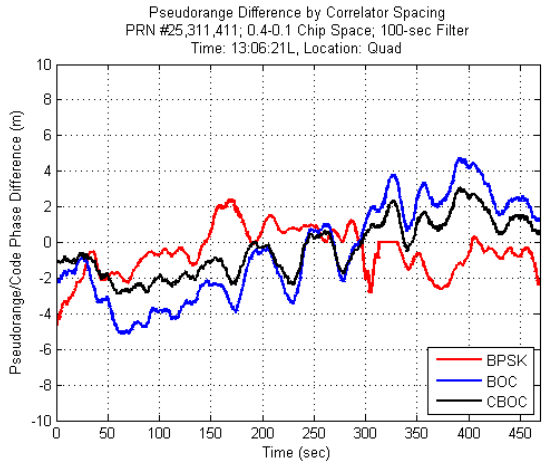

Figure 12: Multipath error comparison between CBOC, BOC, and BPSK in an urban environment

The location under tree foliage presented an extremely difficult scenario to the receiver. Due to the greatly reduced Carrier-to-Noise Ratio (C/No) (approximately 5-15dB), the receiver was often unable to maintain track for several minutes at a time. However, in the data sets taken in the foliage scenario (one shown in Figure 13), the CBOC signal always acquired faster and tracked longer when compared to BOC.

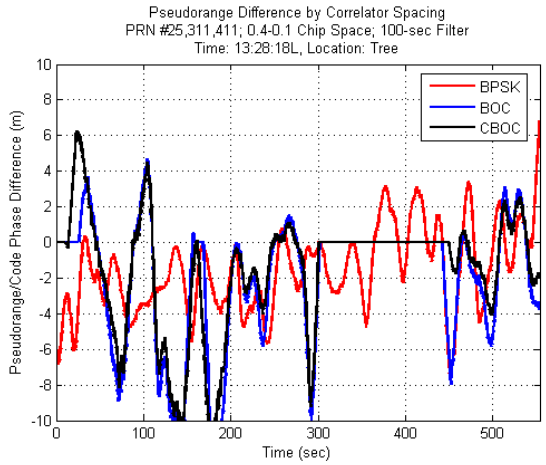

Figure 13: Multipath error comparison between CBOC, BOC, and BPSK while under foliage

As previously mentioned, a 5-15dB drop in C/No was observed when receiving signals under a foliage canopy. Similarly, but to a lesser degree, a 2-8dB drop in C/No was observed when receiving signals in the rooftop courtyard and in the urban environment. At the reference location under open sky conditions, the C/No received from the Galileo and GPS satellites was approximately 48dB and 50dB respectively. This can be seen in Figure 14. In contrast, Figure 15 shows a comparison of received C/No between the Galileo and GPS satellites under foliage and Figure 16 shows the same comparison in the urban environment. It is interesting to note the sinusoidal nature in the C/No plots which suggests the existence of constructive and destructive interference from a multipath signal.

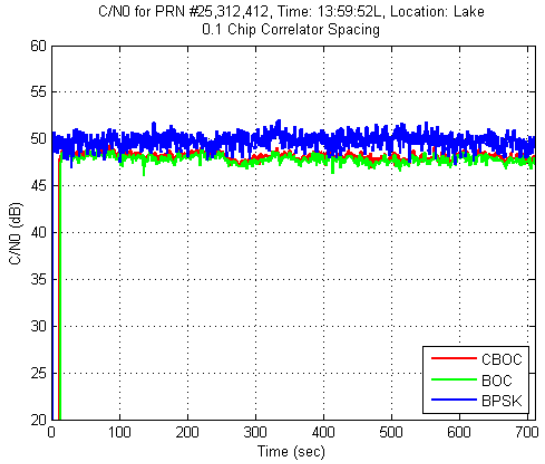

Figure 14: C/No comparison between CBOC, BOC, and BPSK under open skies

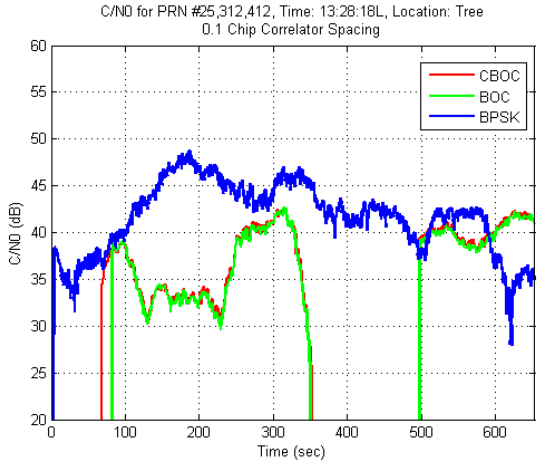

Figure 15: C/No comparison between CBOC, BOC, and BPSK while under foliage

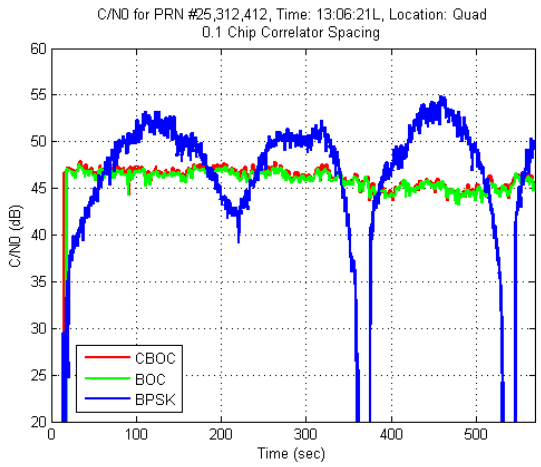

Figure 16: C/No comparison between CBOC, BOC, and BPSK in an urban environment

All eight experiment results show that there is a definitive advantage in the use of CBOC as compared to BOC. However, the comparison between CBOC/BOC and BPSK is less definitive due to the mismatch of satellite geometries. (A few degrees difference in azimuth or elevation makes the difference between catching a tree branch or not). In some experiments, the multipath errors in CBOC/BOC were less than BPSK but about half the time, errors in BPSK were less than CBOC/BOC.

The figures and discussion in this section are only a small subset of the entire dataset resulting from the experiments. The complete series of experiment data is contained in the Appendix

CONCLUSIONS

The experiments described in this paper have shown that the comparison between CBOC/BOC and BPSK was not definitive. Due to the mismatch in satellite geometry, there is no error-free method to compare the multipath geometry seen at the receiver antenna. However, the comparison between CBOC and BOC was definitive. In all scenarios, the CBOC errors were always fully bounded by the BOC errors. In addition, the CBOC tracking loop was consistently able to track quicker and longer in difficult multipath environments (i.e. under tree foliage). Due to the similarities between TMBOC and CBOC (especially when discussing multipath mitigation), it is likely that these results can be extended to a comparison between TMBOC and BOC.

FUTURE WORK

At the time this research was conducted, only two Galileo IOV satellites were in orbit. Since that time, the Galileo program has launched an additional two IOV satellites, making it possible to obtain a position fix during select time windows. Future work would focus on comparing multipath performance in the same or similar scenarios measuring the position error from all satellites rather than the pseudorange error from single satellites.

The proposed methodology would be to calculate the dilution of precision (DOP) of the Galileo constellation at the time of experiment. DOP's for various subsets of visible GPS satellites, each consisting of four satellites, would be calculated in order to best match the current Galileo DOP. The position error, both 2-D and 3-D, would be compared between the Galileo constellation and the best matched GPS constellation subset.

ACKNOWLEDGMENTS

The authors would like to thank the Federal Aviation Administration and Lockheed Martin Space Systems for their continuing generous sponsorship of this research.

In addition, Chiawei Lee would like to thank the Department of Defense SMART Scholarship and the Air Force Test Center, Edwards AFB, CA for their sponsorship of graduate studies at Stanford University.

***Disclaimer**: The opinions or assertions contained herein are the private ones of the author/speaker and are not to be construed as official or reflecting the views of the United States Air Force or Department of Defense.*

REFERENCES

[01] Blanch, J., Walter, T., Enge, P., "A Clock and Ephemeris Algorithm for Dual Frequency SBAS", Proceedings of the 24th International Technical Meeting of The Satellite Division of the Institute of Navigation (ION GNSS 2011), Portland, CA, September 2011.

[02] Hein, G., Betz, J., et al. "MBOC: The New Optimized Spreading Modulation Recommended for GALILEO L1 OS and GPS L1C", ION Plans, 2006.

[03] Braash, M., Van Dierendonck, A.J., "GPS Receiver Architectures and Measurements", Proceedings of the IEEE, Vol. 87, No. 1, January 1999.

[04] Wong, G., Chen, Y.H., Phelts, R.E., Walter, T., Enge, P., "Measuring Code-Phase Differences due to Inter-Satellite Hardware Differences", Proceedings of the 25th International Technical Meeting of The Satellite Division of the Institute of Navigation (ION GNSS 2012), Nashville, TN, September 2012.

[05] Misra, P., Enge P. Global Positioning System: Signals, Measurements, and Performance. Ganga-Jamuna Press, Lincoln, Mass., 2011.

[06] Rouabah, K. et. al., "Unambiguous Multipath Mitigation Technique for BOC(n,n) and MBOC-Modulated GNSS Signals", *International Journal of Antennas and Propagation*, Volume 2012, Article ID 895390.

[07] Intel Corp., "Basic Architecture", In Intel® 64 and IA-32 Architectures Software Developer's Manual, March 2010, Volume 1, Available online: http://www.intel.com/content/www/us/en/processors/architectures-software-developer-manuals.html/ (accessed on 25 July 2012).

[08] Chen, Y.H., Juang, J.C., Seo, J., Lo, S., Akos, D.M., De Lorenzo, D.S., Enge, P., "Design and Implementation of Real-Time Software Radio for Anti-Interference GPS/WAAS Sensors." *Sensors* 12, no. 10: 13417-13440, 2012.

APPENDIX: COMPLETE DATA SETS

In total eight data sets were taken at five different locations from three satellite pairs. The data sets are described in Table 01.

	Location	Satellite Pair
1	Lake Lagunita	Galileo PFM & GPS PRN 25
2	Lake Lagunita	Galileo FM2 & GPS PRN 2
3	Engineering Quad	Galileo PFM & GPS PRN 25
4	Engineering Quad	Galileo FM2 & GPS PRN 2
5	Sculpture Garden	Galileo PFM & GPS PRN 25
6	Sculpture Garden	Galileo FM2 & GPS PRN 2
7	Durand Rooftop	Galileo FM2 & GPS PRN 26
8	Durand Courtyard	Galileo FM2 & GPS PRN 26

Table 01: Dataset Location and Satellite Pairs

For each data set, a pseudorange precision and C/N0 comparison plot was generated.

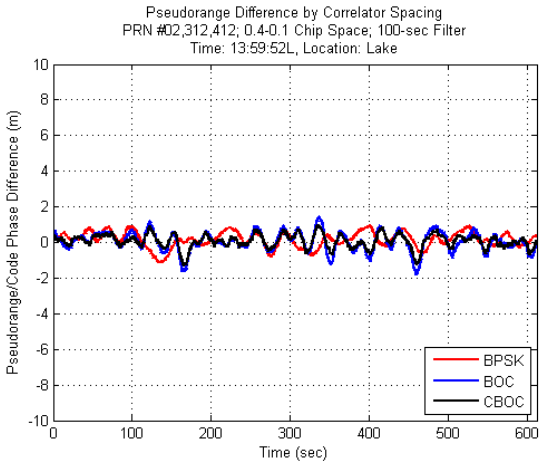

Figure 17: Multipath error comparison between CBOC, BOC, and BPSK (Dataset #1)

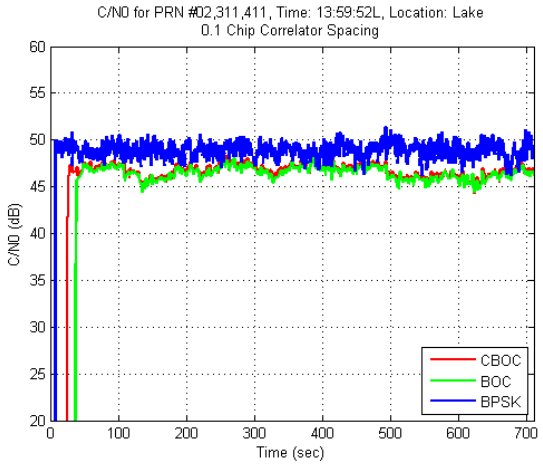

Figure 18: C/N0 comparison between CBOC, BOC, and BPSK (Dataset #1)

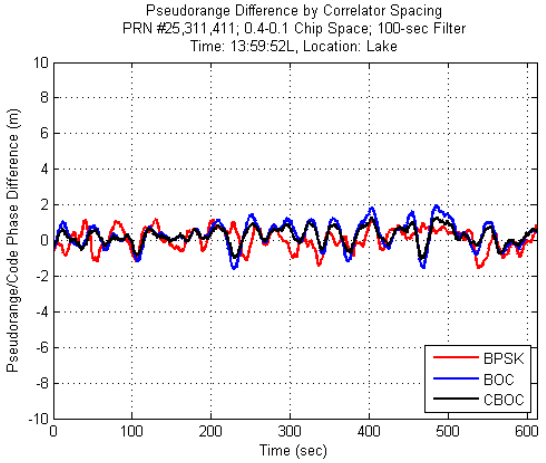

Figure 19: Multipath error comparison between CBOC, BOC, and BPSK (Dataset #2)

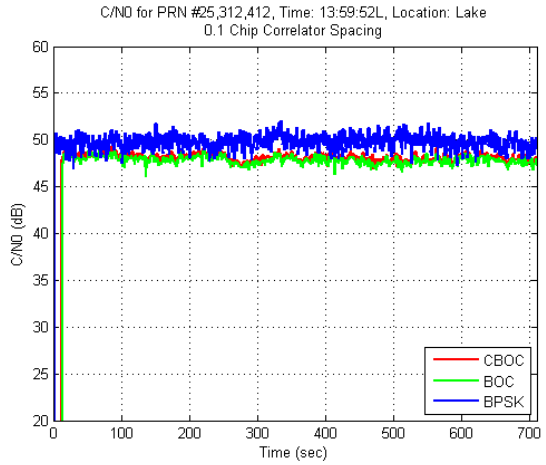

Figure 20: C/N0 comparison between CBOC, BOC, and BPSK (Dataset #2)

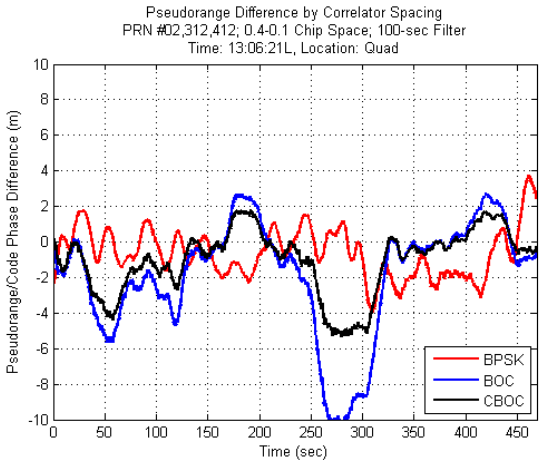

Figure 21: Multipath error comparison between CBOC, BOC, and BPSK (Dataset #3)

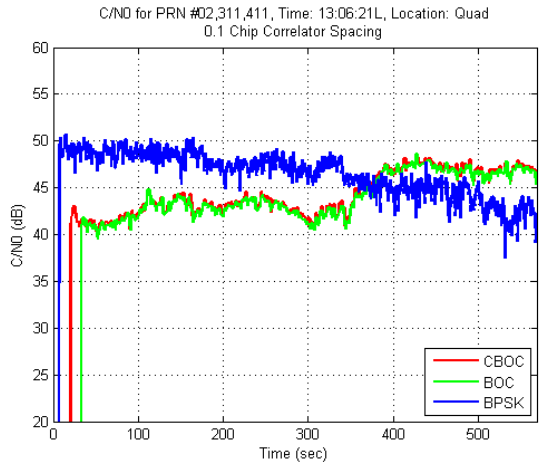

Figure 22: C/N0 comparison between CBOC, BOC, and BPSK (Dataset #3)

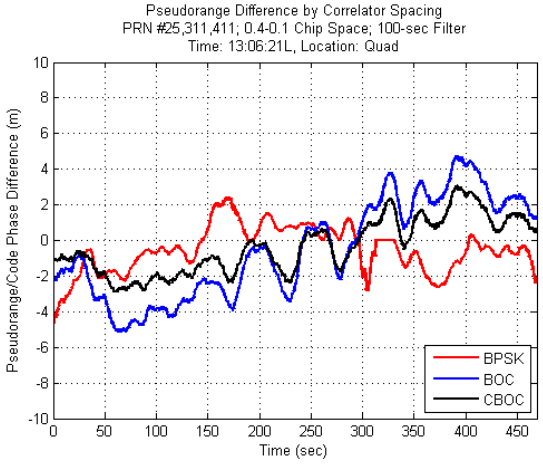

Figure 23: Multipath error comparison between CBOC, BOC, and BPSK (Dataset #4)

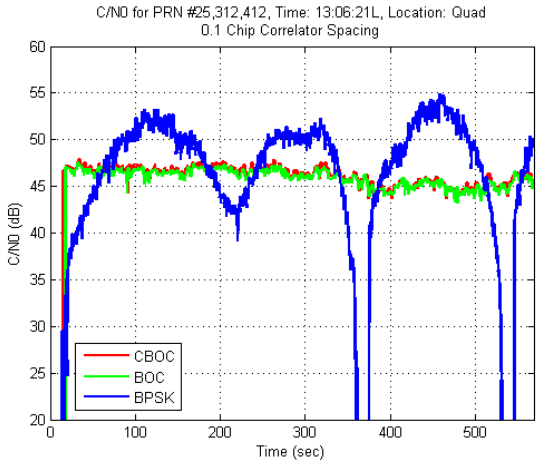

Figure 24: C/N0 comparison between CBOC, BOC, and BPSK (Dataset #4)

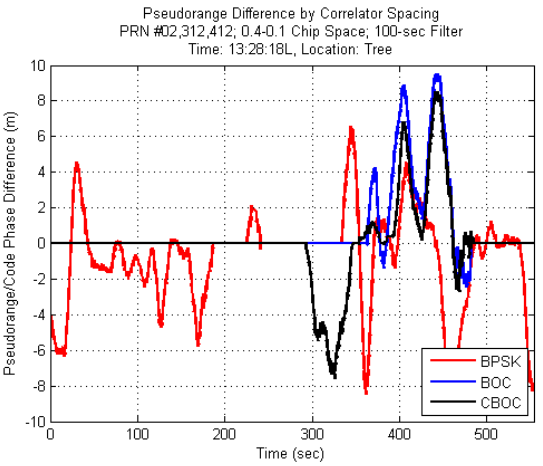

Figure 25: Multipath error comparison between CBOC, BOC, and BPSK (Dataset #5)

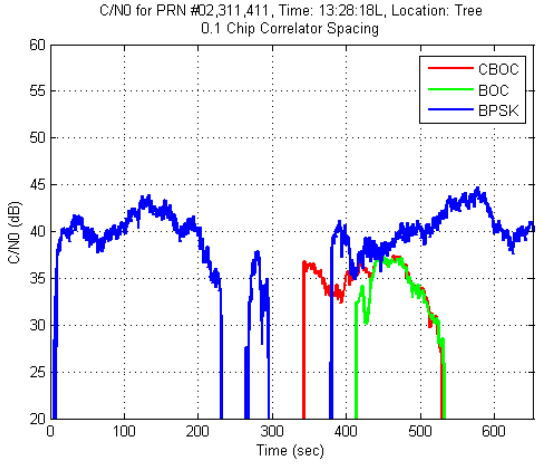

Figure 26: C/N0 comparison between CBOC, BOC, and BPSK (Dataset #5)

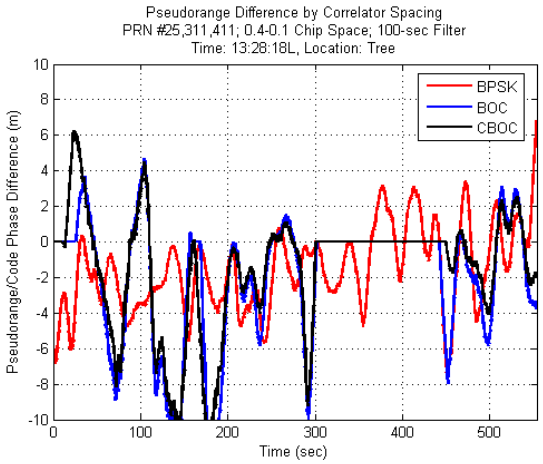

Figure 27: Multipath error comparison between CBOC, BOC, and BPSK (Dataset #6)

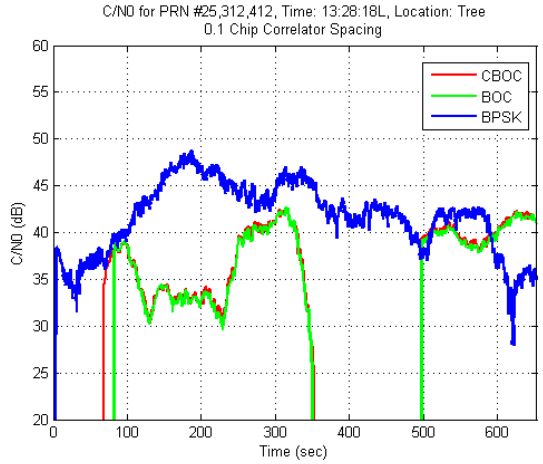

Figure 28: C/N0 comparison between CBOC, BOC, and BPSK (Dataset #6)

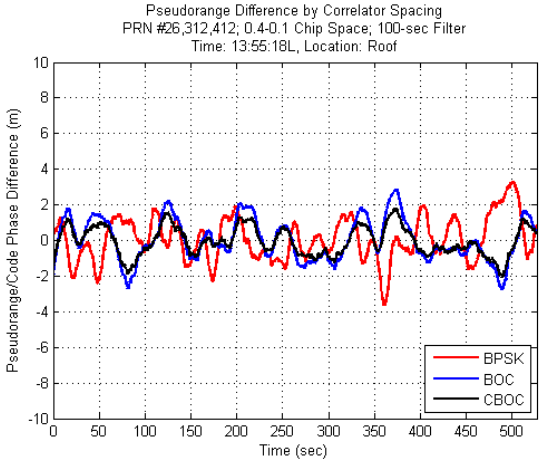

Figure 29: Multipath error comparison between CBOC, BOC, and BPSK (Dataset #7)

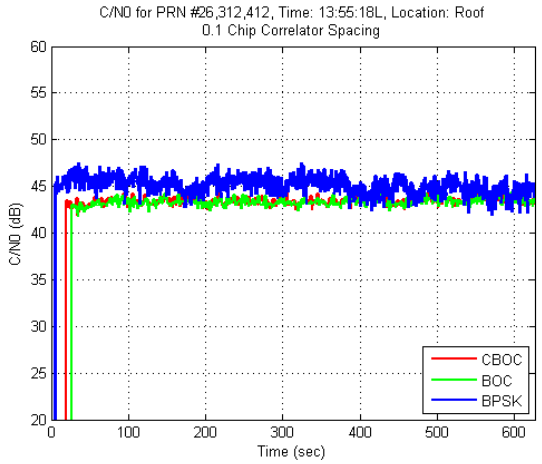

Figure 30: C/N0 comparison between CBOC, BOC, and BPSK (Dataset #7)

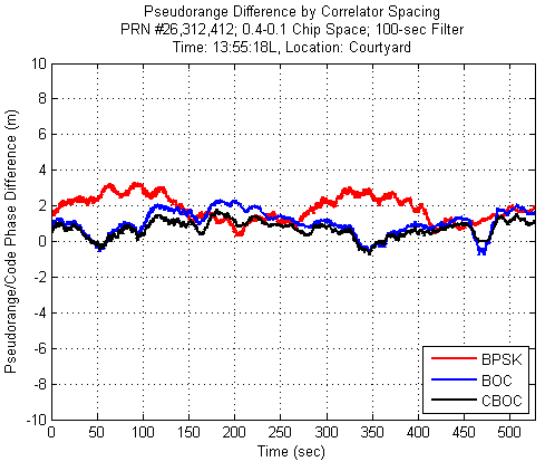

Figure 31: Multipath error comparison between CBOC, BOC, and BPSK (Dataset #8)

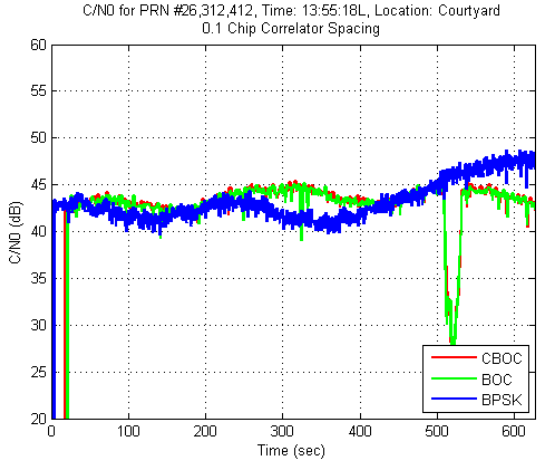

Figure 32: C/N0 comparison between CBOC, BOC, and BPSK (Dataset #8)